ChemComm

COMMUNICATION

View Article Online
View Journal | View Issue



Check for updates

Cite this: *Chem. Commun.*, 2022, **58**, 3318

Received 21st January 2022,
Accepted 10th February 2022

DOI: 10.1039/d2cc00320a

rsc.li/chemcomm

# Organotelluroxane molecular clusters assembled *via* Te···$X^-$ ($X = Cl^-$, $Br^-$) chalcogen bonding anion template interactions†

Andrew Docker,*[a] Antonio J. Martínez Martínez,[b] Heike Kuhn[a] and Paul D. Beer*[a]

**The synthesis and characterisation of two novel molecular organotelluroxane clusters, comprising of an inorganic $Te_8O_6X_4$ (X = Cl, Br) core structure are described. The integration of highly electron withdrawing 3,5-bis-trifluoromethylphenyl groups to the constituent Te(IV) centres is determined to be crucial in the chalcogen bonding (ChB) halide template directed assembly. Characterised by multi-nuclear $^1H$, $^{125}Te$, $^{19}F$ NMR, UV-Vis, IR spectroscopies and X-ray crystal structure analysis, the discrete molecular clusters exhibit excellent organic solvent solubility and remarkable chemical stability. Furthermore, preliminary fluorescence investigations reveal the telluroxanes exhibit aggregation induced emission (AIE) behaviour in organic aqueous solvent mixtures.**

In the construction of large, highly ordered macromolecular assemblies, the use of metal template-directed structural components have featured heavily.[1–3] In particular, transition metal cations possessing predictable coordination geometries and thermodynamically stable complexes have been successfully exploited in generating elaborate and complex molecular topologies.[1,4–7] However, recent years have witnessed exotic sigma-hole based non-covalent interactions, such as halogen bonding (XB) and chalcogen bonding (ChB) being exploited for recognition-derived spontaneous assembly.[8–13] In this context, seminal work by Vargas-Baca and others have elegantly demonstrated that rational and considered incorporation of ChB donor–acceptor arrays in complementary molecular subunits can provide access to a diverse library of impressive, functional supramolecular assemblies.[14–22] Organotelluroxanes, containing highly polar Te–O bonds, have shown enormous promise in this regard,[23,24] frequently displaying intriguing structural behaviour forming oligomeric, polymeric and macrocyclic networks dictated by tellurium centred electrophilic interactions.[25–28] Our own research endeavours have focused on the development of ChB donors and related sigma-hole interactions as anion recognition motifs which through the strategic selection of key structural and electronic factors tune anion binding potency and selectivity.[29–32] Recently, we and others have demonstrated the Lewis acidity of tellurium-based sigma-hole donors is highly sensitive to local electronic environments and can be dramatically enhanced by integration of electron-withdrawing groups, especially when directly bound to the chalcogen atom.[33–36] Motivated by these observations, we sought to establish whether this strategy of increasing Te-based sigma-hole donor potency through electronic polarisation could be exploited in the directed assembly of telluroxane architectures. Herein, we explore the synthesis of new telluroxanes *via* hydrolysis of diaryl tellurium dihalides ($Ar_2TeX_2$, X = Cl, Br), bearing highly electron withdrawing 3,5-bis-trifluoromethylphenyl (Ar) substituents. In the presence of a halide templating agent, a molecular $Ar_{16}Te_8O_6X_4$ cluster is spontaneously formed (Fig. 1). Characterised by a suite of spectroscopic techniques and X-ray diffraction structural analysis, the clusters are comprised of an $Te_8O_6X_4$ core assembled through Te···$X^-$ ($X^-$ = $Cl^-$, $Br^-$) ChB-anion interactions. Notably, the telluroxane clusters exhibit highly desirable physical

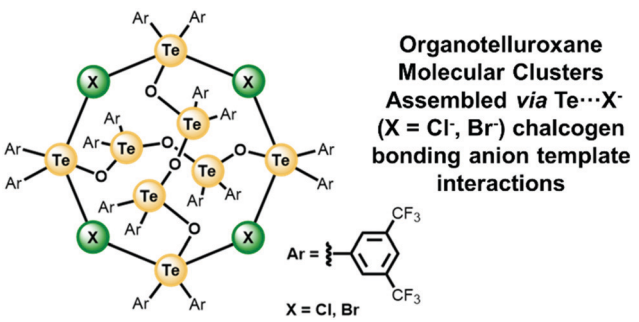


Fig. 1 Chemical structure of $Ar_{16}Te_8O_6X_4$ clusters.

[a] *Chemistry Research Laboratory, Department of Chemistry, University of Oxford, Mansfield Road, Oxford, OX1 3TA, UK. E-mail: andrew.docker@chem.ox.ac.uk, paul.beer@chem.ox.ac.uk*

[b] *Supramolecular Organometallic and Main Group Chemistry Laboratory, CIQSO-Center for Research in Sustainable Chemistry and Department of Chemistry, University of Huelva, Campus El Carmen, ES-21007 Huelva, Spain*

† Electronic supplementary information (ESI) available. CCDC 2131078. For ESI and crystallographic data in CIF or other electronic format see DOI: 10.1039/d2cc00320a

properties, including organic solvent solubility and chemical stability. Furthermore, preliminary photophysical investigations reveal the clusters exhibit aggregation induced emission (AIE) behaviour, becoming highly fluorescent upon the formation of hydrophobically driven aggregates.

The main method employed for the preparation of organotelluroxane compounds is the controlled hydrolysis of their respective diorgano tellurium(IV) dihalide ($Ar_2TeX_2$).[24] With the objective of increasing ChB sigma-hole donor potency, the integration of highly electron withdrawing bis-trifluoromethylphenyl groups as inductively activating aryl appendages to the chalcogen centre was undertaken. Access to the requisite $Ar_2TeX_2$ (X = Cl, Br) species was explored through two routes, A and B, summarised in Scheme 1. Route A involved the treatment of 1,3-bis-trifluoromethylbromo benzene with *n*-BuLi in anhydrous $Et_2O$ at −78 °C, affording the corresponding organolithium species *via* a lithium halogen exchange reaction. Subsequent addition of an anhydrous $Et_2O$ $TeCl_4$ or $TeBr_4$ suspension gave the respective $Ar_2TeX_2$ species. Hydrolysis was achieved by carefully controlled addition of an $NH_4X_{(aq)}$ solution to the crude reaction mixtures. Route B required the of isolation of diaryl telluride **3**, which was obtained by treatment of diaryl ditelluride **2** with a 1 M $Br_2$ $CH_2Cl_2$ solution to afford the corresponding organotellurium bromide, which was reacted immediately with a freshly generated THF solution of 1,3-bis-trifluoromethyl-phenylmagnesium bromide. Oxidative halogenation of **3**, *via* addition of a $Cl_2$ or $Br_2$ $CH_2Cl_2$ solution, afforded the $Ar_2TeX_2$ species which was subjected to an analogous hydrolysis procedure with $NH_4X_{(aq)}$. Identical aqueous work up procedures were undertaken for each of the crude reaction mixtures, in which TLC analysis revealed the formation of one major species. Isolation of these species from the hydrolysis (either Route A or B) of the diorgano tellurium dichloride or dibromide by column chromatography afforded the corresponding products, **1**·Cl and **1·Br**, as highly organic solvent soluble colourless solids. It is noteworthy that analogous reaction conditions in which the hydrolysis of the $Ar_2TeX_2$ species was attempted in the absence of $NH_4X$, gave intractable mixtures of highly insoluble products, and no detectable amounts of the telluroxane cluster products. Furthermore, while routes A and B gave comparable yields of **1**·Cl and **1·Br** (see ESI†), attempts to conduct similar hydrolysis reactions of $Ar_2TeI_2$ (accessible by Route B) gave no isolable product. Inspection of the $^1H$, $^{125}Te$ and $^{19}F$ NMR spectra in acetone-$d_6$ of the isolated products **1**·Cl and **1·Br**, revealed highly similar and relatively simple spectra (Fig. S18a, ESI†). The $^1H$ NMR spectrum showed only two signals, in which integration determined a 1 : 2 ratio, consistent with those belonging to a bis-trifluoromethylphenyl group. The $^{125}Te$ spectra similarly indicated the presence of one resolved signal at *ca.* 820 ppm, consistent with the typical chemical shifts observed for a tellurane (O–$Ar_2Te$–O) and similarly the $^{19}F$ NMR spectra also indicated one resonance corresponding to the trifluoromethyl groups. Importantly, it was also observed that the NMR signals for **1·Cl** or **1·Br** were concentration independent (1–50 mM), implying the absence of non-covalent interactions between the isolated species in solution phase. The UV-Vis spectra of **1·Cl** and **1·Br** exhibited principal absorptions at 262 and 300 nm (Fig. S18b, ESI†), whereas in the IR, a complex profile of the phenyl ring and intense absorptions from the $CF_3$ groups in the region 1350–1000 $cm^{-1}$ were observed. Notably, another distinct sharp absorption at 679 $cm^{-1}$ consistent with the characteristic tellurane (Te–O) stretch was also seen for both **1·Cl** and **1·Br** (Fig. S18c and S15, ESI†).[37] Interestingly, at wavenumbers larger than 1350 $cm^{-1}$, **1·Cl** and **1·Br** demonstrated excellent IR transparency, importantly indicating the absence of hydroxyl functionalities (Fig. 18c, ESI†).[38] ESI-MS analysis of **1·Cl** and **1·Br** revealed the presence of several telluroxane cations including; $[Ar_2TeO]^+$ ($m/z$ = 572.9), $[(Ar_2Te)_2O_2]^+$ ($m/z$ = 1140.8), $[(Ar_2Te)_2O_2]^+$ ($m/z$ = 1140.8) and $[(Ar_2Te)_3O_3]^+$ ($m/z$ = 1712.9), which are presumably the result of autoionization under MS conditions (Fig. S16, ESI†).[28] Determined melting points of **1·Cl** and **1·Br** (47 °C and 49 °C respectively) are in stark contrast with the vast majority of reported telluroxane structures, which typically exhibit high melting points (>100 °C).[26,28,38,39] The combined spectroscopic evidence, such as, resolved concentration independent NMR signals and physical properties including low sharp melting points and excellent solubility in a wide range of non-polar solvents (*e.g.* dichloromethane, hexane, toluene, Fig. S4–S6, ESI†) all suggests that both **1·Cl** and **1·Br** are discrete molecular entities. It is noteworthy that this is contrary to the vast majority of telluroxanes reported to date, which are invariably oligomeric or polymeric structures of largely ionic character.

Crystals of **1·Cl** and **1·Br** suitable for X-ray diffraction analysis were obtained by slow evaporation of chloroform solutions (see ESI† for full discussion of the crystallographic data analysis). Fig. 2 shows both **1·Cl** and **1·Br** exhibit impressive isostructural oblate-shaped cluster structures, consisting of two orthogonally arranged tetratelluroxane chains. These constituent oligotelluroxane chains are comprised of internal ditellurane (O–$TeAr_2$–O–$TeAr_2$–O) and two terminal telluronium ($TeAr_2$–O) units. The terminal Te atoms of the chain are connected to Te termini of the other oligotelluroxane fragment through two halide bridging ligands, generating a macrotricyclic $Te_8O_6X_4$ core. This internal oxotellurium halide network is shielded by an array of exterior bis-trifluoromethylphenyl substituents attached to the Te(IV) centres. Inspection of the telluroxane cluster structures aids the rationalisation of several observations made during their synthesis. Firstly, the absence of any product formation without

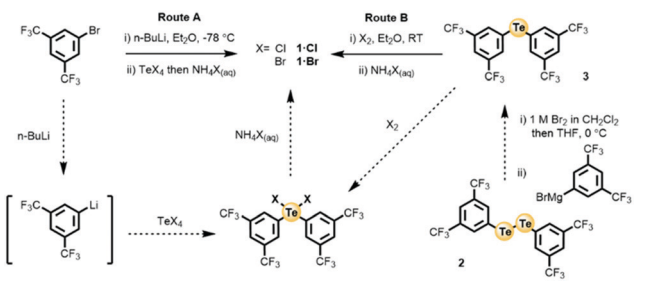


Scheme 1 Synthetic routes A and B to organotelluroxanes **1·Cl** and **1·Br**.

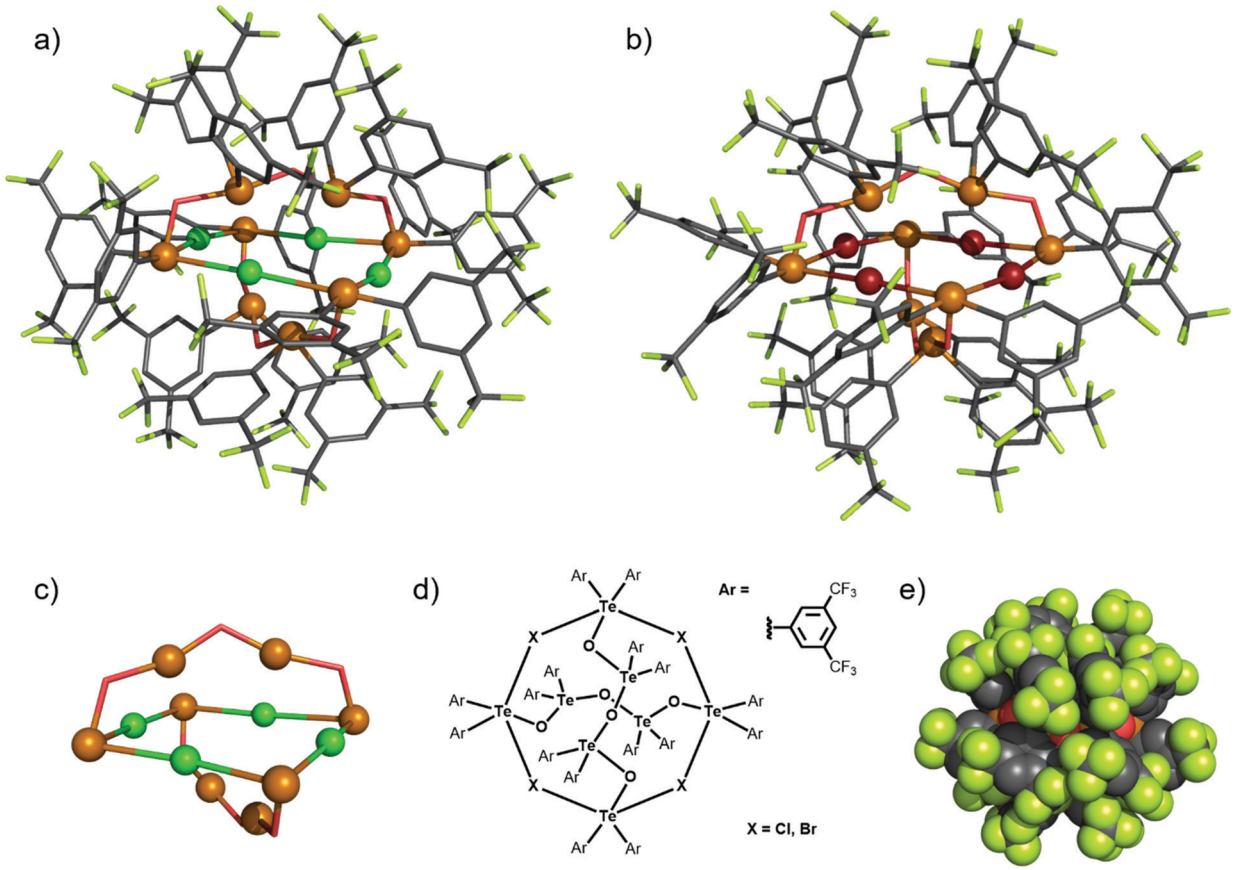


Fig. 2 Solid state structure of (a) **1·Cl** and (b) **1·Br**. (c) Structure of the oxytellurium halide core $Te_8O_6X_4$. (d) Chemical structure of $Ar_{16}Te_8O_6X_4$. (e) Space filling representation of **1·Cl**. Grey = carbon, light green = fluorine, green = chloride, brown = bromine, red = oxygen, orange = tellurium.

the presence of ammonium chloride or bromide, indicates that the cluster assembly is facilitated by a high concentration of chloride or bromide, which is understandable if the halide serves as a templating agent. Presumably, the inability to form an analogous structure with an iodide counteranion is attributed to the decreased anion basicity and/or structural implications imposed on the framework by the larger halide. The high solubility in organic solvents such as hexane and toluene can also be explained, as the polar inorganic oxotellurium halide interior is effectively shielded by multiple fluorinated aromatic residues. Motivated by these findings we sought to investigate if this organic envelopment of the $Te_8O_6X_4$ core conferred stability to the cluster assembly. In this vein, samples of **1·Cl** and **1·Br** were dissolved in $CD_2Cl_2$ to which was added a 10-fold excess of a $AgPF_6$ or $NaBAr^F{}_4$ in $CD_2Cl_2$. Remarkably, the persistent solution homogeneity and negligible difference in the pre- and post- salt addition $^1$H NMR spectra, even after 30 minutes of stirring at room temperature, indicated the cluster structures possess considerable resistance to anion exchange reactions. This may be interpreted as a combination of kinetic inertness, arising from the inaccessibility of the halide containing core, and a thermodynamic penalty from the rupture of a bifurcated ChB–halide bond. Attention subsequently turned to revisiting $^{125}$Te NMR characterisation of the clusters. At 298 K an acetone-$d_6$ solution of **1·Cl** and **1·Br** exhibits a single clearly resolved signal in the $^{125}$Te spectrum, at a chemical shift consistent with a typical tellurane environment. However, the structure as determined by XRD reveals the presence of two tellurium environments, namely the tellurane and telluronium. The absence of a resonance corresponding to the telluronium termini at room temperature conditions is not entirely unexpected and is consistent with numerous reports of oligotelluroxanes.[39] Attempts to observe the characteristically broad telluronium signal by recording the $^{125}$Te spectra of **1·Cl** acetone-$d_6$ at −90 °C did not resolve any additional Te signals (see ESI†), despite high concentrations (50 mM) and long acquisition times (10 hours). Interestingly, the corresponding $^1$H and $^{19}$F NMR spectra at −90 °C, also revealed only minor changes at the low temperature. These low temperature NMR spectroscopic observations suggest that even at −90 °C the rotation of bis-trifluoromethyl aryl substituents is still fast on the $^1$H and $^{19}$F NMR timescales. To further probe the chemical integrity of the clusters, water stability studies were conducted wherein increasing water volumes were added to THF solutions of either **1·Cl** or **1·Br** ($10^{-5}$ M). Importantly, no significant perturbations in the UV-Vis spectrum were observed with increasing water fractions, indicating appreciable cage stability towards hydrolysis. However, during the course of these experiments, it was observed that as the water percentage increased the solutions became increasingly emissive. Intrigued by this behaviour, we

 

sought to investigate the photophysical properties of **1·Cl**, and how they might be affected by aggregation. Preliminary fluorescence studies demonstrated that a THF solution of **1·Cl** ($10^{-5}$ M) is essentially non-emissive ($\lambda_{ex}$ = 350 nm). However, upon increasing the percentage water fraction ($f_w$) of the solution (0–50%), a progressive increase in fluorescence intensity is observed ($\lambda_{max}$ = 350 nm), reaching a dramatic 13-fold increase in emission intensity at $f_w$ = 50% (Fig. S9, ESI†). This type of solvent dependent emission behaviour is characteristic of aggregation induced emissive (AIE) molecules, in which upon aggregation the restriction of intramolecular rotational and or vibrational freedom supresses non-radiative decay pathways, thereby increasing fluorescent output. Analogous experiments conducted with **1·Br** also revealed similar AIE like behaviour, suggesting that the identity of the halide plays little or no role in the cluster's photophysical behaviour.

In conclusion, we report the synthesis of two novel organotelluroxane $Ar_{16}Te_8O_6X_4$ molecular clusters. It is shown that the directed assembly and structural integrity relies upon the formation of potent Te···$X^-$ ($X^-$ = $Cl^-$, $Br^-$) ChB-anion template interactions. Importantly as demonstrated by physical properties, multinuclear NMR characterisation and reactivity studies, the hydrophobic insulation of the inorganic oxotellurium halide core by an organic exterior confers remarkable stability to the cluster framework. In addition, preliminary fluorescence investigations demonstrate **1·Cl** and **1·Br** exhibit AIE behaviour in THF–$H_2O$ mixtures. In the case of **1·Cl** an impressive 13-fold enhancement in emission intensity at a $f_w$ value of 50% is observed. These results serve to illustrate the powerful strategy of exploiting potent ChB–anion interactions in the design and construction of elaborate main-group supramolecular inorganic–organic hypervalent Te(IV) assemblies, potentially displaying a wealth of structural diversity and optical/electronic material properties.

A. D thanks the EPSRC for a studentship (Grant reference number EP/N509711/1). A. J. M. M thanks the MICIN and FEDER (RYC-2017-21783, EUR2020-112189, PID2019-108292RA-I00 and P20-00373) and AIQBE (55-2020).

## Conflicts of interest

There are no conflicts to declare.

## Notes and references

1 S. Leininger, B. Olenyuk and P. J. Stang, *Chem. Rev.*, 2000, **100**, 853–908.
2 J. E. M. Lewis, P. D. Beer, S. J. Loeb and S. M. Goldup, *Chem. Soc. Rev.*, 2017, **46**, 2577–2591.
3 M. Fujita, M. Tominaga, A. Hori and B. Therrien, *Acc. Chem. Res.*, 2005, **38**, 369–378.
4 M. Han, D. M. Engelhard and G. H. Clever, *Chem. Soc. Rev.*, 2014, **43**, 1848–1860.
5 K. K. G. Wong, N. H. Pérez, A. J. P. White and J. E. M. Lewis, *Chem. Commun.*, 2020, **56**, 10453–10456.
6 J. F. Nierengarten, C. O. Dietrich-Buchecker and J. P. Sauvage, *J. Am. Chem. Soc.*, 1994, **116**, 375–376.
7 L. Zhang, D. P. August, J. Zhong, G. F. S. Whitehead, I. J. Vitorica-Yrezabal and D. A. Leigh, *J. Am. Chem. Soc.*, 2018, **140**, 4982–4985.
8 L.-J. Riwar, N. Trapp, K. Root, R. Zenobi and F. Diederich, *Angew. Chem., Int. Ed.*, 2018, **57**, 17259–17264.
9 N. Biot and D. Bonifazi, *Chem. – Eur. J.*, 2018, **24**, 5439–5443.
10 A. Docker, X. Shang, D. Yuan, H. Kuhn, Z. Zhang, J. J. Davis, P. D. Beer and M. J. Langton, *Angew. Chem., Int. Ed.*, 2021, **60**, 19442–19450.
11 K. Kobayashi, H. Izawa, K. Yamaguchi, E. Horn and N. Furukawa, *Chem. Commun.*, 2001, 1428–1429.
12 N. Biot, D. Romito and D. Bonifazi, *Cryst. Growth Des.*, 2021, **21**, 536–543.
13 N. Biot and D. Bonifazi, *Coord. Chem. Rev.*, 2020, **413**, 213243.
14 P. C. Ho, J. Lomax, V. Tomassetti, J. F. Britten and I. Vargas-Baca, *Chem. – Eur. J.*, 2021, **27**, 10849–10853.
15 P. C. Ho, J. Z. Wang, F. Meloni and I. Vargas-Baca, *Coord. Chem. Rev.*, 2020, **422**, 213464.
16 N. A. Puskarevsky, A. I. Smolentsev, A. A. Dmitriev, I. Vargas-Baca, N. P. Gritsan, J. Beckmann and A. V. Zibarev, *Chem. Commun.*, 2020, **56**, 1113–1116.
17 J. Lee, L. M. Lee, Z. Arnott, H. Jenkins, J. F. Britten and I. Vargas-Baca, *New J. Chem.*, 2018, **42**, 10555–10562.
18 N. A. Pushkarevsky, P. A. Petrov, D. S. Grigoriev, A. I. Smolentsev, L. M. Lee, F. Kleemiss, G. E. Salnikov, S. N. Konchenko, I. Vargas-Baca, S. Grabowsky, J. Beckmann and A. V. Zibarev, *Chem. – Eur. J.*, 2017, **23**, 10987–10991.
19 P. C. Ho, H. A. Jenkins, J. F. Britten and I. Vargas-Baca, *Faraday Discuss.*, 2017, **203**, 187–199.
20 P. C. Ho, J. Rafique, J. Lee, L. M. Lee, H. A. Jenkins, J. F. Britten, A. L. Braga and I. Vargas-Baca, *Dalton Trans.*, 2017, **46**, 6570–6579.
21 P. C. Ho, P. Szydlowski, J. Sinclair, P. J. W. Elder, J. Kübel, C. Gendy, L. M. Lee, H. Jenkins, J. F. Britten, D. R. Morim and I. Vargas-Baca, *Nat. Commun.*, 2016, **7**, 11299.
22 P. C. Ho, V. Tomassetti, J. F. Britten and I. Vargas-Baca, *Inorg. Chem.*, 2021, **60**, 16726–16733.
23 J. Beckmann and P. Finke, in *Selenium Tellurium Chemistry Small Molecules Biomolecules Materials*, ed. J. D. Woollins, R. Laitinen, Springer, Berlin, Heidelberg, 2011, pp. 151–177.
24 K. Srivastava, A. Panda, S. Sharma and H. B. Singh, *J. Organomet. Chem.*, 2018, **861**, 174–206.
25 T. M. Klapötke, B. Krumm, P. Mayer and O. P. Ruscitti, *Z. Naturforsch., B: J. Chem. Sci.*, 2002, **57**, 145–150.
26 K. Srivastava, S. Sharma, H. B. Singh, U. P. Singh and R. J. Butcher, *Chem. Commun.*, 2010, **46**, 1130–1132.
27 H. Citeau, K. Kirschbaum, O. Conrad and D. M. Giolando, *Chem. Commun.*, 2001, 2006–2007.
28 L. Kirsten, J. F. Rodrigues, A. Hagenbach, A. Springer, N. R. Pineda, P. C. Piquini, M. R. Jungfer, E. S. Lang and U. Abram, *Angew. Chem.*, 2021, **133**, 15645–15651.
29 A. Docker, T. Bunchuay, M. Ahrens, A. J. Martinez-Martinez and P. D. Beer, *Chem. – Eur. J.*, 2021, **27**, 7837–7841.
30 Y. C. Tse, A. Docker, Z. Zhang and P. D. Beer, *Chem. Commun.*, 2021, **57**, 4950–4953.
31 L. E. Bickerton, A. Docker, A. J. Sterling, H. Kuhn, F. Duarte, P. D. Beer and M. J. Langton, *Chem. – Eur. J.*, 2021, **27**, 11738–11745.
32 A. Docker, J. G. Stevens and P. D. Beer, *Chem. – Eur. J.*, 2021, **27**, 14600–14604.
33 T. Bunchuay, A. Docker, U. Eiamprasert, P. Surawatanawong, A. Brown and P. D. Beer, *Angew. Chem., Int. Ed.*, 2020, **59**, 12007–12012.
34 A. Docker, C. H. Guthrie, H. Kuhn and P. D. Beer, *Angew. Chem., Int. Ed.*, 2021, **60**, 21973–21978.
35 B. Zhou and F. P. Gabbaï, *Chem. Sci.*, 2020, **11**, 7495–7500.
36 B. Zhou and F. P. Gabbaï, *J. Am. Chem. Soc.*, 2021, **143**, 8625–8630.
37 N. W. Alcock and W. D. Harrison, *J. Chem. Soc., Dalton Trans.*, 1982, 1421–1428.
38 R. Deka, A. Sarkar, R. J. Butcher, P. C. Junk, D. R. Turner, G. B. Deacon and H. B. Singh, *Dalton Trans.*, 2020, **49**, 1173–1180.
39 J. Beckmann, J. Bolsinger and A. Duthie, *Chem. – Eur. J.*, 2011, **17**, 930–940.